A novel magnetic palladium catalyst for the mild aerobic oxidation of 5-hydroxymethylfurfural into 2,5-furandicarboxylic acid in water

Journal:	*Catalysis Science & Technology*
Manuscript ID:	CY-ART-10-2014-001407.R2
Article Type:	Paper
Date Submitted by the Author:	06-Mar-2015

Complete List of Authors:	Mei, Nan; South-Central University for Nationalities, key Laboratory of Catalysis and Material Sciences of the State Ethnic Affairs Commission & Ministry of Education Liu, Bing; South-Central University for Nationalities, key Laboratory of Catalysis and Material Sciences of the State Ethnic Affairs Commission & Ministry of Education Zheng, Judun; South-Central University for Nationalities, key Laboratory of Catalysis and Material Sciences of the State Ethnic Affairs Commission & Ministry of Education Lv, Kangle; South-Central University for Nationalities, key Laboratory of Catalysis and Material Sciences of the State Ethnic Affairs Commission & Ministry of Education Tang, Dingguo; South-Central University for Nationalities, key Laboratory of Catalysis and Material Sciences of the State Ethnic Affairs Commission & Ministry of Education Zhang, Zehui; South-Central University for Nationalities, key Laboratory of Catalysis and Material Sciences of the State Ethnic Affairs Commission & Ministry of Education

ARTICLE TYPE

Cite this: DOI: 10.1039/c0xx00000x

www.rsc.org/xxxxxx

A novel magnetic palladium catalyst for the mild aerobic oxidation of 5-hydroxymethylfurfural into 2,5-furandicarboxylic acid in water

Nan Mei, Bing Liu,* Judun Zheng, Kangle Lv, Dingguo Tang and Zehui, Zhang*

Received (in XXX, XXX) Xth XXXXXXXXX 20XX, Accepted Xth XXXXXXXXX 20XX

DOI: 10.1039/b000000x

In this study, magnetically separable graphene oxide supported palladium nanoparticles (C-Fe_3O_4-Pd) was successfully prepared via a one-step solvothermal route. The C-Fe_3O_4-Pd catalyst showed excellent catalytic performance in the aerobic oxidation of 5-hydroxymethylfurfural (HMF) into 2,5-furandicarboxylic acid (FDCA). It was found that the base concentration and the reaction temperature significantly affected both HMF conversion and FDCA selectivity. High HMF conversion (98.2%) and FDCA yield (91.8%) were obtained after 4 h at 80 ^oC with K_2CO_3/HMF molar ratio of 0.5. The C-Fe_3O_4-Pd catalyst could be easily collected by an external magnet and reused without the significant loss of its catalytic activity. The developed method is a green and sustainable process for the production of valuable FDCA from renewable bio-based HMF in terms of the use of water as solvent, the requirement of stoichiometric base, the high activity under atmospheric oxygen pressure and the facile recycle of the catalyst.

Introduction

Currently, there is a growing concern in the word on the gradual depletion of fossil oil reservoirs and the awareness of climate change. [1, 2] Much effort has been devoted to the search of renewable resources as alternative to fossil resource to supply chemicals and fuels. Biomass consists mainly of carbohydrate components such as starch, cellulose, and hemicelluloses, which is the only carbon-containing renewable resource. It is not only abundant in the earth but also keeps the carbon balance. Through biorefinery, biomass can be converted into useful chemicals and valuable fuel. [3-5]

Among a range of potential platform compounds, 5-hydroxymethylfurfural (HMF) can be generated by acid-catalyzed dehydration of C6-sugar monomers.[6-9] It has been identified as a versatile platform chemical with high potential for the synthesis of valuable chemicals and liquid fuels.[10] Recently, selective oxidation of HMF is of particular interest, since it can produce several important chemicals such as 2,5-diformylfuran (DFF), 5-hydroxymethyl-2-furancarboxylic acid (HMFCA) and 2,5-furandicarboxylic acid (FDCA) (Scheme 1).[11-13] FDCA has been identified as one of the top 12 value-added chemicals from biomass by the U.S. Department of Energy. It has a similar structure with terephthalic acid, thus it has high potential as a substitute for terephthalic acid for the manufacture of poly(ethylene terephthalate) (PET) plastics.[14] Therefore, there is a growing attention on the synthesis of FDCA by the oxidation of HMF.

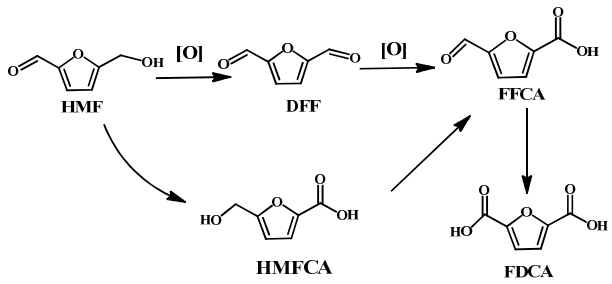

Scheme 1. Major oxidation products from the oxidation of HMF

Department of Chemistry, Key Laboratory of Catalysis and Material Sciences of the State Ethnic Affairs Commission & Ministry of Education.
South-Central University for Nationalities
MinYuan Road 182, Wuhan, R.P. China
E-mail:liubing@mail.scuec.edu.cn;
zhangzehui@mail.scuec.edu.cn;

The oxidation of HMF into FDCA has been performed under different reaction conditions using both homogeneous and heterogeneous catalysts. In early work, the combined $Co^{2+}/Mn^{2+}/Br^-$ catalysts were used for the oxidation of HMF into FDCA in acetic acid at 125 ^oC under 70 bar air pressure.[15] As it is difficult to recycle homogeneous catalysts, researchers mainly focused on the development of new heterogeneous catalysts for the oxidation of HMF into FDCA. In most cases, inorganic materials supported Pt, Pd, Ru and Au nanoparticles have been used as heterogeneous catalysts for the aerobic oxidation of HMF into FDCA. For example, Davis et al. reported that Pd/C and Pt/C catalysts could promote the full oxidation of HMF with FDCA yields between 71% and 79% with NaOH/HMF mole ratio of 2 under 690 kPa O_2 pressure.[16] Supported Au nanoparticles have shown encouraging catalytic performance for the aerobic oxidation of HMF to FDCA in water, and have been received great interest.[17-21] However, the stability of the supported Au catalysts in the aerobic oxidation of HMF remains a problem. For example, Corma et al. reported that CeO_2-supported Au nanoparticles (CeO_2/Au) showed high catalytic activity for the oxidation of HMF to FDCA with a high yield of 99% at 130 ^oC under 1 MPa air pressure and high concentration of NaOH (4 equiv of HMF), but the activity of CeO_2/Au in the second run declined sharply.[17] In addition, most of the currently reported methods required the use of high base amount (with 2~20 mole ratio of HMF) and high oxygen pressure. Acknowledging these important achievements, the quest for milder and greener methodologies for selective oxidation of HMF into FDCA still remains a great challenge.

In recent years, graphene-based materials such as graphene and graphene oxide (GO) have shown important applications in various fields such as electrochemistry, electronics, biochemistry, and hydrogen storage.[22] The graphene-based materials have also been received an extensive attention as a promising support to stabilize nanoparticles including metals and metal oxides by strong π-interaction between the nanoparticles with its supported carbon nanosheets.[23]Among them, graphene oxide-Fe_3O_4 nanoparticles, which is formed by the decoration of Fe_3O_4 on the graphene oxide, has particularly been attracted as an excellent carbonaceous support in catalyst and separation fields due to the facile recovery by an external magnet. [24]

Recently, the use of palladium nanoparticles has been attracted strong interest owing to the high catalytic activity compared to the bulk phase.[25] In order to prevent the aggregation of palladium nanoparticles, several kinds of supports have been used to immobilize the palladium nanoparticles. However, the recycle of supported palladium nanoparticles suffers from the need of cost- and time-intensive filtration methods. One effective method to solve this problem is the application of magnetic supports, which allow the recovery of Pd nanoparticles by simple decantation in the presence of an external magnet.[26,27] In an attempt to develop a green and sustainable method for the oxidation of HMF into FDCA under mild conditions, the above mentioned graphene-magnetite nanocomposite promoted us to use it as a supporting material for the immobilization of palladium nanoparticles, which can act as a magnetically separable catalyst for the oxidation of HMF into FDCA.

Experimental Section

Materials

Ethylene glycol (99.5%), $FeCl_3.6H_2O$ (99.5%), sodium acetate (NaOAc, 99.5%), NaOH (99.5%), $NaNO_3$ (99.5%) and $KMnO_4$ (99.5%) were purchased from Sinopharm Chemical Reagent Co., Ltd. (Shanghai, China). HCl (36.5%) and H_2SO_4 (98.0%) was purchased from Kaifeng Chemical Reagent Co., Ltd. (Kaifeng, China). Graphite powder and Sodium tetrachloropalladate(II) (Na_2PdCl_4, 98%) were purchased from Aladdin Chemicals Co. Ltd. (Beijing, China). HMF (98%) was purchased by Beijing Chemicals Co. Ltd. (Beijing, China). DFF (98%) and FDCA (97.0%) were purchased from the J&K Chemical Co. Ltd., (Beijing, China). Acetonitrile (HPLC grade) was purchased from Tedia Co. (Fairfield, USA). All the solvents were purchased from Sinopharm Chemical Reagent Co., Ltd. (Shanghai, China).

Preparation of graphene oxide

Graphite oxide was prepared by a modified Hummer's method.[28] Graphite (3.0 g) and $NaNO_3$ (2.25 g) were added into a 1000 mL beaker in an ice bath. Then 98.0 wt.% H_2SO_4 (225 mL) was added into the beaker with a vigorous stirring for 30 min. Then $KMnO_4$ (13.5 g) were added into the mixture slowly over 2 h. After the addition of $KMnO_4$, the mixture was stirred for 2 h at 0 ^oC, subsequently at 25 °C for 5 days. After that, the temperature was raised to 98 ^oC and 5 wt.% H_2SO_4 (450 mL) was added dropwise for 1 h. Then, the mixture was stirred at 98 ^oC for 2 h. The temperature was then reduced to 25 ^oC and the mixture was stirred for another 2 h. Finally, the solid product was collected by centrifugation, and washed 15 times with 3 wt.% H_2SO_4, followed by 5 times with 3 wt.% HCl. Finally, the solid product was in a vacuum oven at 40 ^oC to obtain graphite oxide.

Synthesis of C-Fe_3O_4-Pd composite

30 mg of graphite oxide was added to 10 mL of water, and the mixture was subjected to the sonication for 30 min in order to make graphite oxide homogeneously disperse into water. 20 mL of ethylene glycol was then added to the above mixture, followed by sonication for additional 30 min. Then, $FeCl_3.6H_2O$ (0.1 g) and NaOAc (1.2 g) were added to a mixed solvent of water (5 mL) and ethylene glycol (10 mL), then the mixture was stirred at room temperature for 1 h to obtain a clear solution. The as-prepared clear solution was added dropwise to the graphite oxide solution, and then the mixture was stirred for 30 min. Then, Na_2PdCl_4 (4 mg) dissolved in 5 mL of *N,N*-dimethylformamide was added dropwise and the mixture was stirred for another 30 min. Finally, the mixture was transferred into an autoclave, and kept stillness at 130 ^oC for 14 h. After cooling to room temperature, the catalyst was collected by an external magnet, washed with water and ethanol, dried in a vacuum oven at 40 ^oC. Finally, 37 mg of the black catalyst was obtained, which was abbreviated as C-Fe_3O_4-Pd.

Catalyst characterization

Transmission electron microscope (TEM) images were obtained using an FEI Tecnai G^2-20 instrument. The sample powder were firstly dispersed in ethanol and dropped onto copper grids for observation. X-ray powder diffraction (XRD) patterns of samples

were determined with a Bruker advanced D8 powder diffractometer (Cu Kα). All XRD patterns were collected in the 2θ range of 10–80° with a scanning rate of 0.016°/s. X-ray photoelectron spectroscopy (XPS) was conducted on a Thermo VG scientific ESCA MultiLab-2000 spectrometer with a monochromatized Al Kα source (1486.6 eV) at constant analyzer pass energy of 25 eV. The binding energy was estimated to be accurate within 0.2 eV. All binding energies (BEs) were corrected referencing to the C1s (284.6 eV) peak of the contamination carbon as an internal standard. FT-IR measurements were recorded on a Nicolet NEXUS-6700 FTIR spectrometer with a spectral resolution of 4 cm^{-1} in the wave number range of 500-4000 cm^{-1}. The Pd content in the C-Fe_3O_4-Pd catalyst was quantitatively determined by inductively coupled atomic emission spectrometer (ICP-AES) on an IRIS Intrepid II XSP instrument (Thermo Electron Corporation). Magnetization measurement was performed by using a physical property measurement system (PPMS-9T) with VSM option from Quantum Design. Applied magnetic fields H between -30 and 30 kOe and temperature 300 K were used in the experiments.

Determination of Pd loading by ICP-AES

The palladium content in the C-Fe_3O_4-Pd catalyst was quantitatively determined by inductively coupled atomic emission spectrometer (ICP-AES) on an IRIS Intrepid II XSP instrument (Thermo Electron Corporation). The acid digestion was composed of concentrated HNO_3 (7.5 mL), 48 wt.% HF (1.5 mL) and 2.5 mL concentrated HCl (2.5 mL). 0.5 g sample was digested in the above acid digestion on the flat electric furnace. After digestion, the sample was diluted with deionized water and centrifuged at 3,000 rpm. The supernatant liquid was subjected to ICP-AES analysis. The ICP-AES operation conditions were as follows: Incident power: 1.1 KW, carrier gas flow rate: 0.8 L min^{-1}, auxiliary gas flow rate: 0.4 L min^{-1}, coolant gas flow rate: 16 L min^{-1}, observation height: 10 mm.

General procedure for the aerobic oxidation of HMF

Typically: HMF (50.4 mg, 0.4 mmol) was firstly dissolved in water (8 mL), then K_2CO_3 (27.6 mg, 0.2 mmol) and C-Fe_3O_4-Pd (40 mg, Pd/HMF mol ratio = 1.8%) were added in the above reaction solution. Then oxygen was flushed at a rate of 20 mL min^{-1}, and the reaction was carried out at 80 °C with a stirring at a constant rate of 600 revolutions per minute (rpm) equipped with a condenser. After reaction, the catalyst was removed, and the reaction solution was diluted with water to a certain volume in each case.

Analytic methods

Furan compounds were analyzed by a ProStar 210 HPLC system equipped with a UV detector. Furan compounds were well separated by a reversed-phase C18 column (200 × 4.6 mm) at the wavelength of 280 nm. Acetonitrile and 0.1 wt.% acetic acid aqueous solution with the volume ratio of 30:70 were used as mobile phase at a flow rate of 1.0 mL/min. The amounts of HMF and FDCA in samples were obtained directly by interpolation from calibration curves.

HMF conversion and FDCA yield are defined as follows:

HMF conversion = moles of HMF/moles of starting HMF×100%

FDCA yield = moles of FDCA/moles of starting HMF ×100%

Catalyst recycling

After reaction, the C-Fe_3O_4-Pd catalyst was collected by a permanent magnet, and the liquid solution was decanted. Then, the spent catalyst was washed with water three times and ethanol twice. Finally, it was dried under vacuum at 50 °C overnight. The spent catalyst was reused for the next run, and other steps were the same.

Results and Discussion

Catalyst preparation and characterization

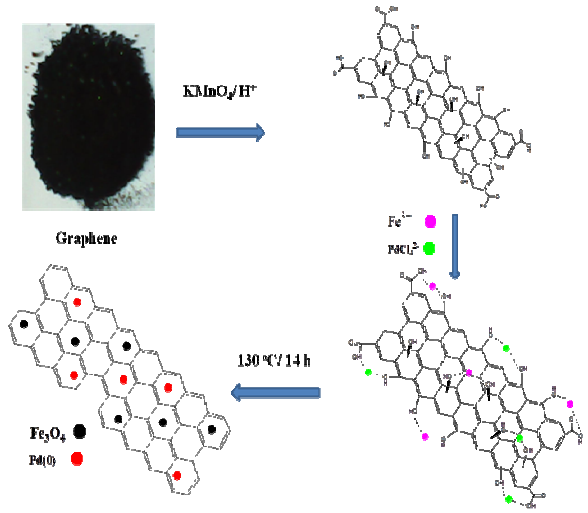

Scheme 2. Schematic illustration of the catalyst preparation.

Scheme 2 shows the procedure of the preparation of the C-Fe_3O_4-Pd catalyst. Firstly, graphite oxide was prepared by the oxidation of pristine graphite by a modified Hummer's method. Both Pd^{2+} and Fe^{3+} ions were then simultaneously anchored on the surface of graphene oxide by π-bonding[29] or ionic interaction between the oxy-functional groups of graphene oxide with corresponding positive charge of the metal ions.[30] Then the metal cations immobilized on graphene oxide were solvothermally reduced to graphene-Fe_3O_4-Pd nanocomposite by ethylene glycol at 130 °C for 14 h.[31] The C-Fe_3O_4-Pd catalyst was readily purified by an external magnet. The Pd content was determined to be 1.95 wt.% by ICP-AES analysis, which meant 1 g of the catalyst contained 19.5 mg of Pd.

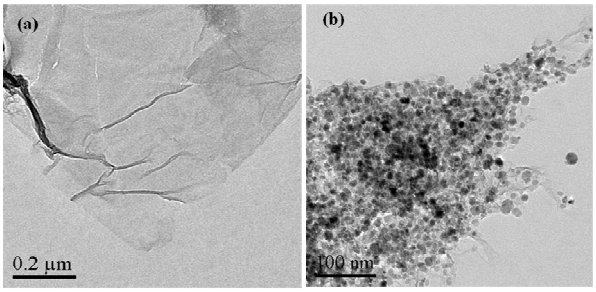

Fig. 1 TEM images of graphite oxide (a) and C-Fe_3O_4-Pd (b).

The heterostructure of the C-Fe_3O_4-Pd catalyst can be verified by the morphological analyses. Fig. 1 showed shows the typical TEM images of graphite oxide and the C-Fe_3O_4-Pd catalyst. As shown in Fig. 1 (a), the folding nature of graphite oxide is clearly visible. On the other hand, graphene oxide had the layer structure, which is believed to be composed of plenty of individual sheets. As shown in Fig. 1(b), the surface of graphene oxide was decorated by the palladium and Fe_3O_4 nanoparticles, and almost no particles scattered out of the supports, which indicated that there was a strong interaction between nanoparticles and support.[29] The morphologies of those nanoparticles were almost regular in nature, and most of them were quite spherical with an average diameter of 10 nm. In addition, as the density and the color of Fe_3O_4 are close to Pd nanoparticles, it was difficult to discriminate Fe_3O_4 and Pd nanoparticles in the C- Fe_3O_4-Pd catalyst. The C-Fe_3O_4-Pd catalyst was well dispersed in water as similar as reported by Yu et al.,[33] which was beneficial to the contact between the substrate and the catalyst sites for chemical reactions in water.

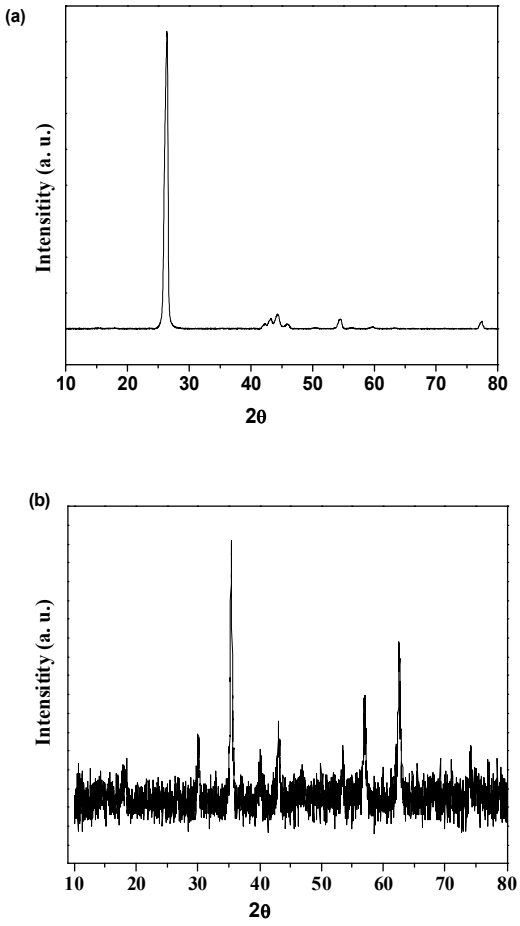

Fig. 2 XRD diffraction patterns of (a) graphite and (b) the C-Fe_3O_4-Pd catalyst.

XRD patterns of the graphite and the C-Fe_3O_4-Pd catalyst are shown in Fig. 2. A strong XRD peak at $2\theta = 26.4^o$ was observed in graphite (Fig. 2 a), which is the characteristic XRD peak of graphite and can be assigned to hexagonal crystalline graphite (JCPDS No. 41–1487).[34] As shown in Fig. 2 (b), after chemical oxidation of graphite by $KMnO_4$, the strong peak at $2\theta = 26.4^o$ was disappeared in the spectrum of C-Fe_3O_4-Pd catalyst, revealing the successful oxidation of the starting graphite.[30] However, no obvious diffraction peaks of graphite oxide were observed in the XRD patterns of the C-Fe_3O_4-Pd catalyst. It is reported that if the regular stacks of graphite oxide was destroyed, for example, by exfoliation, their diffraction peaks were disappeared.[36] The diffraction peaks at $2\theta = 30.1^o$, 35.4^o, 43.1^o, 56.9^o, and 63.2^o were assigned to the reflections of Fe_3O_4, which matched well with the standards of Fe_3O_4 (JCPDS 65-3107). In addition, the peak at $2\theta = 40.1^o$ was also clearly observed, which was attributed to the interplanar-spacing for the (111) of Pd(0) nanoparticles.[33] Seeing from the XRD results, it is confirmed that Fe_3O_4 and Pd (0) nanoparticles were successfully immobilized on the surface of the graphene oxide.

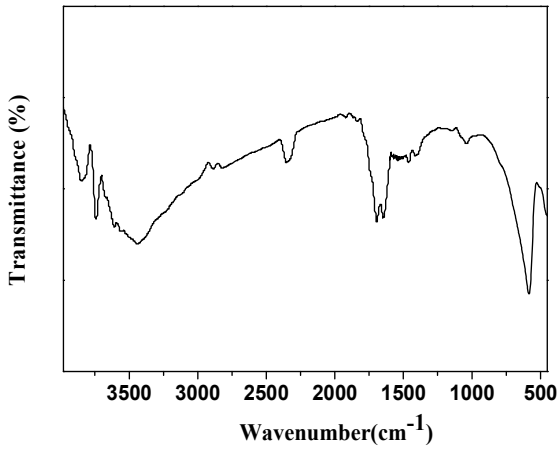

Fig. 3. FT-IR spectra of the C-Fe_3O_4-Pd catalyst.

FT-IR is one of the most important methods to study the oxidation of graphite to graphite oxide. Fig. 3 shows the FT-IR spectra of the C-Fe_3O_4-Pd catalyst. As shown in Fig. 3, several functional groups were appeared after the chemical oxidation of graphite such as –OH (3396 cm^{-1}), –COOH (1725 cm^{-1}), C–O (1058 cm^{-1}) and C=O (1622 cm^{-1}). These functional groups clearly indicated that the graphite was successfully oxidized by $KMnO_4$. The functional groups in graphene oxide have a strong tendency to interact with metal cations with it enhanced hydroxyl and carboxyl group. In addition, a peak at 582 cm^{-1} was also observed, which was assigned to Fe–O vibrations of the Fe_3O_4.[34]

The XPS survey scan spectra of the C-Fe_3O_4-Pd catalyst and Pd 3d region is shown in Fig. 4. These peaks with a binding energy of about 285, 531, and 711 eV were attributed to C 1s, O 1s, and Fe 2p, respectively (Fig. 4 a). In addition, a weak peak with the centre around 335 eV was also observed, which was assigned to Pd 3d. In the case of Fe 2p, two peaks of Fe $2p_{3/2}$ and Fe $2p_{1/2}$ were located at 711.9 and 725.3 eV, respectively, which were the characteristic XPS peaks of Fe^{2+} in Fe_3O_4.[38] In order to

give clear information of the Pd valence, high resolution XPS spectra of Pd 3d was also collected (Fig. 4 b). The binding energy of Pd $3d_{3/2}$ and Pd $3d_{5/2}$ were 335.2 eV and 340.4 eV, respectively. The two peaks were the characteristic peaks of Pd (0), which was in agreement with the previous report,[39] suggesting that the absorbed Pd(II) in the graphene oxide was successfully reduced to Pd(0) nanoparticles under solvothermal reduction. Taking the XPS results together with the information of XRD into consideration, Fe_3O_4 and Pd (0) were successfully decorated on the surface of graphene oxide.

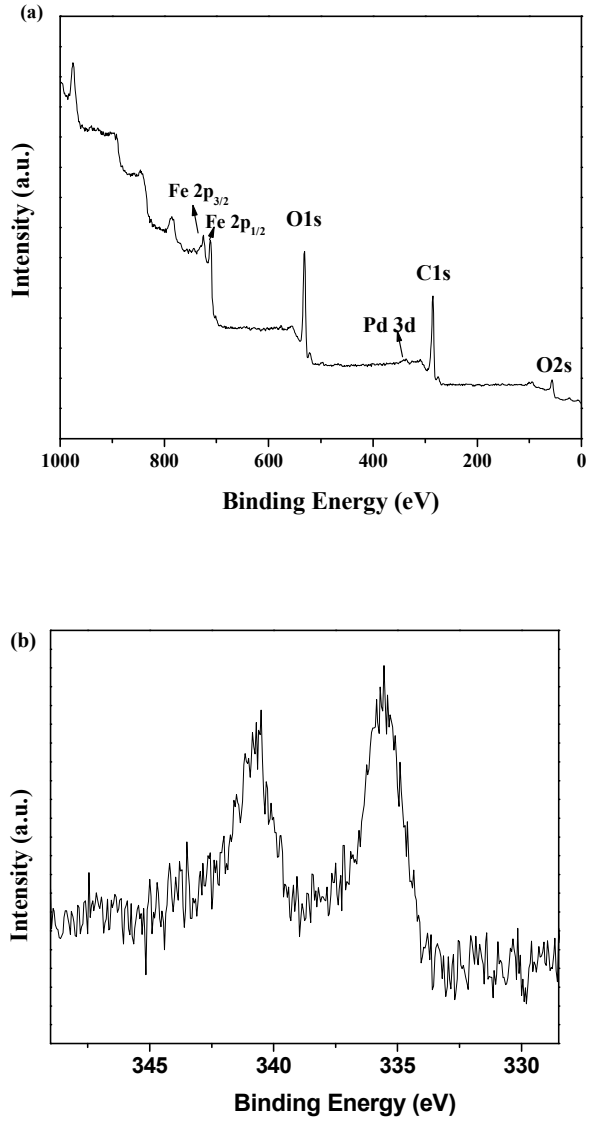

Fig. 4. XPS spectra of the samples. (a) Survey scan of the C-Fe_3O_4-Pd catalyst; (b) Pd 3d region.

As a magnetic catalyst, it should possess sufficient paramagnetic properties for practical applications. Therefore, vibrating sample magnetometer (VSM) analysis was used to test the magnetic property of the C-Fe_3O_4-Pd catalyst, and the magnetic curve of the C-Fe_3O_4-Pd catalyst is shown in Fig. 5. The isothermal magnetization curve of the C-Fe_3O_4-Pd catalyst at 300 K with the field sweeping from −30000 to +30000 Oe displayed a rapid increase with increasing applied magnetic field due to superparamagnetic relaxation. The saturation magnetization was 28.75 emu/g. Therefore, the magnetization of C-Fe_3O_4-Pd catalyst is strong enough for the magnetic separation by a permanent magnet as shown in Fig. 6.

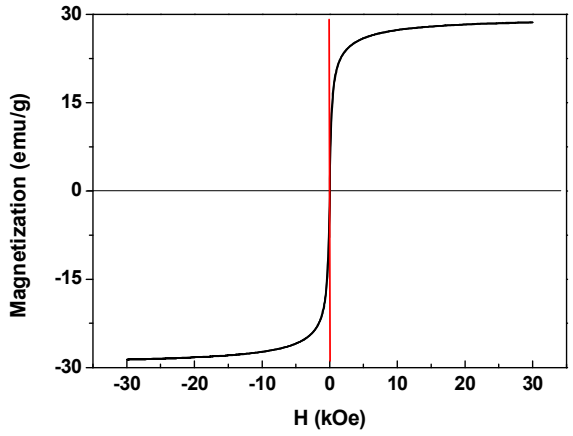

Fig. 5. Hysteresis loops for the C-Fe_3O_4-Pd catalyst at 300 K

Aerobic oxidation of HMF over C-Fe_3O_4-Pd catalyst in various solvents

In previous reports, some methods used organic solvents for the oxidation of alcohols using Pd based catalys,[40] while others used water as the solvent for the oxdation of alcohols.[41] Those reports indicated that the solvent played a crucial role on chemical reactions. Indeed, different solvents have different properties such as the polarity, dielectric constant, steric hindrance, acid-base property, which affect the efficiency of chemical reactions.[42] In addition, it is reported that the supported metal nanoparticles may be deactivated by the formed organic products such as carboxylic acid. Thus, base is usually required to timely neutralize the produced carboxylic acid to keep the catalyst active.[43] Therefore, the oxidation of HMF over C-Fe_3O_4-Pd catalyst was initially carried out in some common solvents using 0.5 equiv of K_2CO_3 as additive. As shown in Table 1, the reaction solvent greatly affected both on HMF conversion and products selectivity. Generally speaking, HMF conversion and the total selectivity of the furan products were higher in polar solvents than those obtained in the solvents with low polarity such as toluene and MIBK. One of the main reasons should be that the base K_2CO_3 and the product FDCA showed poor solubility in toluene and MIBK. Thus, the formed FDCA could not timely be neutralized by K_2CO_3, but absorbed on the catalyst surface, leading to the low catalytic activity. It is interesting to note that different products were produced in DMSO at different reaction temperatures (Table 1, Entries 3 *vs* 4). DFF yield of 30.0% and HMFCA yield of 10.4% were obtained in DMSO at 80 ^oC (Table 1, Entry 3). However, FDCA was the major product with a yield of 45.8% in DMSO when the reaction temperature was increased to 100 ^oC (Table 1, Entry 4). Seeing the results in Entries 3 & 4, DFF and HMFCA should be the intermediates during the

oxidation of HMF into FDCA at 100 °C in DMSO. Among all of the testing organic solvents, C-Fe_3O_4-Pd showed the best catalytic performance in the protic solvent ethanol with HMF conversion of 61.2% and FDCA yield of 50.4% (Table 1, Entry 5). To our pleasure, water was proved to the best solvent for the oxidation of HMF into FDCA over the C-Fe_3O_4-Pd catalyst (Table 1, Entry 6). High HMF conversion of 87.2% and FDCA yield of 82.3% were achieved in water in the presence of 0.5 equiv of K_2CO_3. The oxidation of HMF using water as green solvent with molecular oxygen as the oxidant appears very appealing due to its low cost and without toxic pollution. Control experiment was also conducted by the oxidation of HMF in water without K_2CO_3. As expected, the C-Fe_3O_4-Pd catalyst showed poor catalytic performance in water without K_2CO_3 (Table 1, Entries 6 *vs* 7), confirming the crucial role of base in obtaining excellent catalytic activity of the C-Fe_3O_4-Pd catalyst for the aerobic oxidation of HMF into FDCA in water. It is also interesting to note that not only each solvent gave different products distribution, but also the total furan selectivity was different in each solvent. The lowest total selectivity was observed in toluene and the highest total selectivity was obtained in water.

Table 1 The results of the aerobic oxidation of HMF in different solvents.[a]

Entry	Solvent	HMF Con. (%)	FDCA yield (%)	DFF yield (%)	HMFCA yield (%)	Total Sel. of Furans (%) [d]
1	Toluene	9.2	2.0	3.5	0.9	75.0
2	MIBK	21.9	16.2	2.3	0.4	86.3
3	DMSO	50.6	0	30.0	14.1	87.2
4[b]	DMSO	52.7	45.8	1.4	0.9	91.3
5	Ethanol	61.2	50.4	3.8	1.2	90.5
6	H_2O	87.2	82.3	1.2	0.9	96.8
7[c]	H_2O	12.1	11.1	0.5	0.4	99.2

[a] Reaction conditions: HMF (50.4 mg, 0.4 mmol), solvent (8 mL), C-Fe_3O_4-Pd (40 mg, 1.8 mol.%), K_2CO_3 (27.6 mg, 0.2 mmol), oxygen flow rate (30 mL min^{-1}), 80 °C, 4 h.

[b] The reaction temperature was 100 °C. Otherwise reaction conditions were the same as described above.

[c] The reaction was carried out without K_2CO_3.

[d] Total selectivity of furans were defined as the mole ratio of furan products including FDCA, DFF and HMFCA to the consumed HMF.

Effect of base amount on the aerobic oxidation of HMF into FDCA in water

Table 2 The results of HMF oxidation with different amount of K_2CO_3.[a]

Entry	Mole ratio of K_2CO_3 to HMF	HMF conversion (%)	FDCA yield (%)	FDCA selectivity (%)
1	0.5	87.2	82.3	94.4
2	1.0	98.7	87.6	88.8
3	1.5	100	62.7	62.7
4	0.25	45.4	40.1	88.4
5	0.125	23.8	21.9	92.0
6	0	12.1	11.1	91.7

[a] Reaction conditions: HMF (50.4 mg, 0.4 mmol), H_2O (8 mL), C-Fe_3O_4-Pd (40 mg, 1.8 mol.%), a set amount of K_2CO_3, oxygen flow rate (30 mL min^{-1}), 80 °C, 4 h.

As disscussed above, K_2CO_3 played a crucial role in the aerobic oxidation of HMF over C-Fe_3O_4-Pd catalyst, therefore, the effect of base amount on this reaction were studied. Compared with the results by the use of 0.5 equiv of K_2CO_3 (Table 2, Entry 1), HMF conversion and FDCA yield increased to 98.7% and 87.6% by the use of 1 equiv of K_2CO_3, respectively (Table 2, Entry 2). It is calculated that FDCA selectivity by the use of 1 equiv of K_2CO_3 was a little lower than that obtained with 0.5 equiv of K_2CO_3 (Table 2, Entries 1 *vs* 2). It should be noted that K_2CO_3 also played a negative effect on this reaction, as HMF is not stable under acidic and alkaline conditions. For example, Rass et al. also found that the treatment HMF in Na_2CO_3 (2 equiv) aqueous solution at 100 °C yielded 50% HMF degradation after 2 h.[44] Further increasing the amount of K_2CO_3 to 1.5 equiv, this trend was much more apparent. Full HMF conversion was obtained with FDCA yield of 62.7% by the use of 1.5 equiv of K_2CO_3 (Table 2, Entry 3). As 0.5 equiv of K_2CO_3 was the stoichiometric dosage to neutralize the resultant FDCA in theory, the final reaction solution with 1 and 1.5 equiv of K_2CO_3 was alkaline. When the amount of K_2CO_3 was below 0.5 equiv, HMF conversion and FDCA yield gradually decreased with the decrease of K_2CO_3 (Table 2, Entries 4~6). For example, HMF conversions were 45.4% and 23.8% by the use of 0.25 and 0.125 equiv of K_2CO_3, respectively, and the corresponding FDCA yields were 40.1% and 21.9%, respectively. The reason was that K_2CO_3 was not sufficient to neutralize the product FDCA, resulting in the loss of the activity of the catalyst during reaction process.

Effect of reaction temperature on the aerobic oxidation of HMF

The effect of reaction temperature was also studied for the oxidation of HMF over C-Fe_3O_4-Pd catalyst. Experiments were carried out at four different reaction temperatures in the range from 298 K to 373 K. As shown in Table 3, the aerobic oxidation of HMF was sensitive to the reaction temperature. HMF

conversion and FDCA yield increased with an increase of reaction temperature from 298 K to 353 K (Table 3, Entries 1, 3 & 4). For example, HMF conversion of 41.3% and FDCA yield of 38.3% were obatined at the reaction temperature of 25 ^{o}C (Table 3, Entry 1). Increasing the reaction temperature to 60 ^{o}C greatly enhanced the reaction efficiency, leading to HMF conversion of 77.6% and FDCA yield of 71.1% (Table 3, Entry 3). Futher increasing the reaction temperature to 80 ^{o}C, HMF converion and FDCA yield still improved to 87.2% and 82.3%, respectively (Table 3, Entry 4). It is intresting to note that the selectivity of FDCA was almost the same around 90%, indicating that the side reaction especially base-promoted degradation of HMF was not serious in the reaction temperature range from 298 K to 353 K. HMF conversion further increased from 87.2% at 80 ^{o}C to 97.1% at 100 ^{o}C (Table 3, Entries 4 & 5). However, FDCA yield of 80.5% at 100 ^{o}C was a little lower than that at 80 ^{o}C (Table 3, Entries 4 *vs* 5). The main reason should be that the base-promoted degradation of HMF became more serious at a higher reaction temperature. For instance, Rass et al. reported that up to 50% HMF was degraded into other byproducts after 2 h at 100 ^{o}C in Na_2CO_3 (2 equiv) aqueous solution.[44] It is worth noting that high HMF conversion of 95.4% and FDCA yield of 87.9% could be achieved at room temperature (25 ^{o}C) after prolonging the reaction time from 4 h to 12 h (Table 3, Entry 2). To the best of our knowledge, there is no report on the oxidation of HMF into FDCA under such mild reaction conditions (eg. room temperature, atmospheric oxygen pressure, low dosage of base).

Table 3 The results of HMF oxidation at different reaction temperatures. [a]

Entry	Temperature (^{o}C)	HMF conversion (%)	FDCA yield (%)	FDCA selectivity (%)
1	25	41.3	38.3	92.7
2[b]	25	95.4	87.9	92.1
3	60	77.6	71.1	91.6
4	80	87.2	82.3	94.4
5	100	97.1	80.5	82.9

[a] Reaction conditions: HMF (50.4 mg, 0.4 mmol), H_2O (8 mL), C-Fe_3O_4-Pd (40 mg, 1.8 mol%), K_2CO_3 (27.6 mg, 0.2 mmol), oxygen flow rate (30 mL min^{-1}), 4 h.
[b] The reaction time was 12 h under otherwise the same reaction conditions as described above

Aerobic oxidation of HMF with different catalyst amounts

Experiments were also carried out with different amounts of the catalyst to investigate the effect of catalyst loading. Table 4 shows the results of HMF conversion, FDCA yield and selectivity. Generally, the larger the catalyst dosage was, the higher the HMF conversion and FDCA yield were (Table 4, Entries 1~3). HMF conversion of 57.8% and FDCA yield of 52.9% were obtained after 4 h using 20 mg of C-Fe_3O_4-Pd (Table 4, Entry 1).

Table 4 The results of HMF oxidation with different catalyst loading. [a]

Entry	Time (h)	Catalyst amount	HMF conversion (%)	FDCA yield (%)	FDCA selectivity (%)
1	4	20 mg, 0.9 mmol%	57.8	52.9	91.5
2	4	40 mg, 1.8 mol%	87.2	82.3	94.4
3	4	60 mg, 2.7 mol%	98.2	91.8	93.5
4[b]	4	40 mg, 1.8 mol%	47.7	43.9	92.0
5[b]	12	40 mg, 1.8 mol%	94.4	85.7	90.8
6[c]	4	60 mg, 2.7 mol%	13.0	0	0

[a] Reaction conditions: HMF (50.4 mg, 0.4 mmol), a certain amount of the C-Fe_3O_4-Pd catalyst, water (8 mL), K_2CO_3 (27.6 mg, 0.2 mmol), oxygen flow rate (30 mL min^{-1}), 80 ^{o}C, 4 h.
[b] The reaction was carried in the air. Otherwise reaction conditions were the same above.
[c] Gaphene oxide-Fe_3O_4 was used as the catalyst for the same reaction.

It is noted that increasing catalyst dosage to 40 mg resulted in a sharp increase of HMF conversion (87.2%) and FDCA (82.3%) (Table 4, Entry 2). The increase of HMF conversion with an increase of catalyst dosage at the same reaction time should be attributed to an increase in the availability and number of catalytically active sites. Further increasing catalyst amount to 60 mg, HMF conversion continually increased from 87.2% to 98.2%, and the corresponding FDCA yield was 91.8% (Table 4, Entry 3). It is worth noting that the selectivity of FDCA was almost the same in each case, suggesting that it had no direct relation with the catalyst amount. As discussed above, the main side reaction was caused by the base-promoted degradation of HMF, which mainly depended on the base concentration and reaction temperature. The high catalytic activity of C-Fe_3O_4-Pd inspired us to carry out the reaction in the air without the flush of oxygen. To our delights, good results were also observed for the oxidation of HMF in the air. HMF conversion of 47.7% and FDCA yield of 43.9% were obtained after 4 h in the air, which were lower than that with the flush of oxygen (Table 4, Entries 2 *vs* 4). The reason should be that the concentration of oxygen in the reaction solution in air was lower than that with the flush of oxygen. After prolonging the reaction time to 12 h, oxidation of HMF in the air also afforded an excellent FDCA yield of 85.7% (Table 4, Entry 5). The excellent results of the aerobic oxidation of HMF in the

air made this method easily handy and economic in the practical application. Control experiments were also carried out by the use of graphene oxide-Fe_3O_4 as the catalyst, which was prepared by the same method of the C-Fe_3O_4-Pd catalyst without the addition of Na_2PdCl_4 during the preparative procedure. No FDCA was determined in the oxidation of HMF over graphene oxide-Fe_3O_4 catalyst (Table 4, Entry 6), which indicated that Pd nanoparticles were the active sites for the oxidation of HMF into FDCA. The conversion of HMF in Entry 6 was caused by the base-promoted degradation of HMF into other byproducts.

Catalyst recycling experiments and large-scale reaction

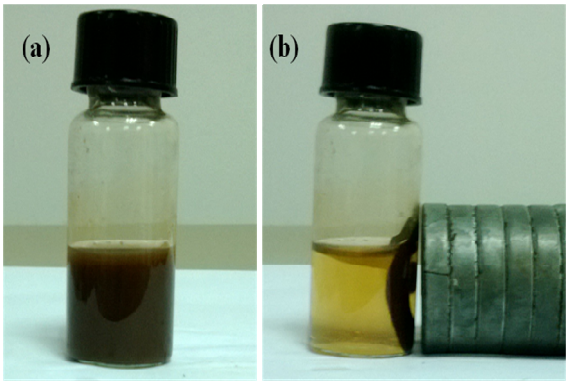

Fig. 6 Separation of the catalyst simply by a magnet. (a) After reaction; (b) Separation by an external magnet.

As a magnetic catalyst, the facile recycle of the catalyst and the high stability should be the important characteristics. Therefore, experiments on catalyst recycling were also studied. As shown in Fig. 6, after reaction, the C-Fe_3O_4-Pd catalyst was easily collected from the reaction mixture by a permanent magnet. Then the liquid solution was decanted, and the spent catalyst was washed with water three times and ethanol twice. Finally, the spent catalyst was dried under vacuum at 50 ^oC overnight. Then the spent catalyst was used for the second run under the same reaction conditions as described for the first run. As shown in Fig. 7, FDCA yield were almost the same near about 91%. There results indicated that the C-Fe_3O_4-Pd catalyst was stable during the reaction process without the loss of its catalytic activity. In addition, the stability of the catalyst was also confirmed by ICP-AES. The reaction solution was subjected to be analyzed by ICP-AES. No palladium was determined in the reaction solution, which indicated that there was no leach of palladium from the catalyst to the reaction solution. The stability of the prepared C-Fe_3O_4-Pd catalyst was the same as that reported by Villa et al. [45]. They used active carbon supported bi-metallic nanoparticles (Au_8Pd_2/AC) for the oxidation of HMF into FDCA, and found that it was stable during the recycle experiment.

Finally, the large-scale oxidation of HMF into FDCA was also carried out. 1 g of HMF was used as the starting material. As the reaction required to neutralize the formed FDCA, 0.5 equiv of Na_2CO_3 (0.55 g) was also used. 1 g of HMF and 0.55 g of Na_2CO_3 were added into 100 mL of water, and then the reaction was carried out at 80 ^oC by the use of 0.5 g of C-Fe_3O_4-Pd with oxygen flow rate at 30 mL min^{-1}. Thin lay chromatography was used to track the reaction process. After 12 h reaction, HMF was completely disappeared. Then, the catalyst was removed, and the reaction solution was concentrated by reduce evaporation. Then the resulting residues were purified on silica gel, eluting with methanol/ethyl acetate. The amount of isolated FDCA 1.05 g, equaling to a yield of 84.8%. Compared with the above microreaction, the yield of large scale reaction was a little lower.

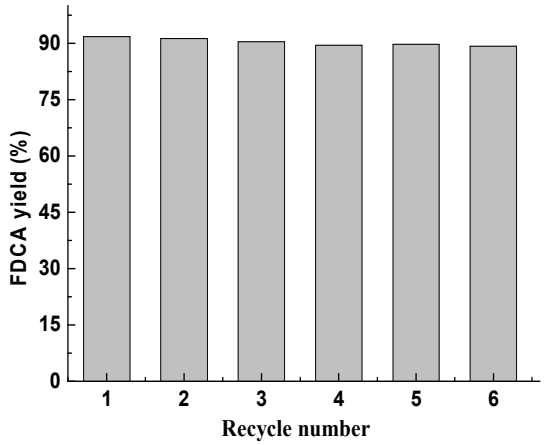

Fig. 7 Recycle experiments of the C-Fe_3O_4-Pd catalyst. Reaction conditions: HMF (50.4 mg, 0.4 mmol), H_2O (8 mL), K_2CO_3 (27.6 mg, 0.2 mmol), oxygen flow rate (30 mL min^{-1}), C-Fe_3O_4-Pd (60 mg, 2.7 mol%), 80 ^oC, 4 h.

Conclusion

In this study, superparamagnetic C-Fe_3O_4-Pd catalyst was successfully prepared by the one-pot solvothermal route and it showed high catalytic activity in the aerobic oxidation of HMF into FDCA in water under mild reaction conditions. Results demonstrated that reaction temperature and base concentration greatly affected the oxidation of HMF, but also the degradation of HMF. Under optimal reaction conditions, high HMF conversion of 98.2% and FDCA yield of 91.8% were obtained after 4 h at 80 ^oC with K_2CO_3/HMF molar ratio of 0.5. Excellent results could also been achieved by the oxidation of HMF over C-Fe_3O_4-Pd catalyst in the air or at room temperature with an appropriate reaction time. More importantly, the catalyst could be easily recovered by an external magnet, and reused without the loss of its catalytic activity. Compared with other reported methods, the present catalytic system showed three distinct advantages such as the use of stoichiometric amount of base, the high activity under atmospheric oxygen pressure and the facile catalyst recycle. It is believed that this finding will provide an efficient method for the production of other valuable chemicals by the oxidation of various biomass-derived hydroxyl compounds in a green and sustainable method.

Acknowledgements

The Project was supported by National Natural Science Foundation of China (No. 21203252, & No. 21206200), the Chenguang Youth Science and Technology Project of Wuhan

City (No. 2014070404010212), and the Natural Science Foundation of Hubei Province (no. 2014CFB180).

References

1 F. Rizzi, N. J. van Eck and M. Frey, *Renew. Energ.* 2014, **62**, 657-671.

2 A. J. Ragauskas, C. K. Williams, B. H. Davison, G. Britovsek, J. Cairney, C. A. Eckert, W. J. Frederick, J. P. Hallett, D. J. Leak, C. L. Liotta, J. R. Mielenz, R. Murphy, R. Templer and T. Tschaplinski, *Science* 2006, 311, 484-489.

3 Y. Xiong, Z. H. Zhang, X. Wang, B. Liu and J.T. Lin, *Chem. Eng. J.* 2014, **235**, 349-355.

4 S. Pickard, S. S. Daood, M. Pourkashanian and W, Nimmo, *Fuel* 2014, **134,** 171-179.

5 I. Agirrezabal-Telleria, I. Gandarias and P. L. Arias, Catal. Today 2014, **234**, 42-58.

6 Z. H. Zhang, Q. Wang, H. B. Xie, W. J. Liu and Z. K. Zhao, *ChemSusChem* 2011, **4**, 131-138.

7 L. Hu, G. Zhao, X. Tang, Z. Wu, J. X. Xu, L. Lin and S. J. Liu *Bioresource Technol.* 2013, **148**, 501-507

8 T. F. Wang, M. W. Nolte, and B. H. Shanks, *Green Chem.* 2014, **16**, 548-572.

9 S. H. Xiao, B. Liu, Y. M. Wang, Z. F. Fang and Z. H. Zhang, *Bioresource Technol.* 2014, **151**, 361–366.

10 R. -J. van Putten, J. C. van der Waal, E. de Jong, C. B. Rasrendra, H. J. Heeres and J. G. de Vries, *Chem. Rev.* 2013, **113**, 1499-1597.

11 B. Liu, Z. H. Zhang, K. L. Lv, K. J. Deng and H. M. Duan, *Appl. Catal. A-Gel*. 2014, **472**, 64-71.

12 G. S. Yi, S. P. Teong, X. K. Li and Y. G. Zhang, *ChemSusChem* 2014, 7, 2131-2135.

13 Z. H. Zhang, Z. L. Yuan, D. G. Tang, Y. S. Ren, K. L. Lv and B. Liu, *ChemSusChem* 2014, **7**, 3496-3504.

14 C. H. R. M. Wilsens, B. A. J. Noordover and S. Rastogi, Polymer, 2014, 55, 2432-2439.

15 B. Saha, S. Dutta and M. M. Abu-Omar, *Catal. Sci. Technol.* 2012, **2**, 79-81.

16 S. E. Davis, L. R. Houk, E. C. Tamargo, A. K. Datye and R. J. Davis, *Catal. Today*, 2011, **160**, 55–60.

17 O. Casanova and A. Corma, *ChemSusChem* 2009, **2**, 1138−1144.

18 N. Guppta, S. Nishimura, A. Takagaki and K. Ebitani, *Green Chem*. 2011, **13**, 824−827.

19 S. Davis, B. Zope and R. Davis, *Green Chem*. 2012, **14**, 143−147.

20 J. Cai, H. Ma, J. Zhang, Q. Song, Z. Du, Y. Huang and J. Xu, *Chem. Eur. J*. 2013, **19**, 14215−14223.

21 A. Villa, M Schiavoni, S Campisi, G. M. Veith and L. Prati, *ChemSusChem* 2013, **6**, 609-612.

22 S. Navalon, A. Dhakshinamoorthy, M. Alvaro and H. Garcia, *Chem. Rev.* 2014, **114**, 6179−6212

23 R. Hao, W. Qian, L. Zhang and Y. Hou, *Chem. Commun.* 2008, **45**, 6576-6578.

24 J. Huang, Q. Chang, Y. B. Ding, X. Y. Han and H. Q. Tang, *Chem. Eng. J.* 2014, **254**, 434-442.

25 Z. H. Zhang, J. D. Zhen, B. Liu, K. L. Lv and K. J. Deng, *Green. Chem.* 2015, **17**, 1308-1317.

26 R. Linhardt, Q. M. Kainz, R. N. Grass, W. J. Stark and O. Reiser, *RSC Adv*. 2014, **4**, 8541-8549.

27 Q. M. Kainz, R. Linhardt, R. N. Grass, G. Vile, J. Perez-Ramirez, W. J. Stark, O. Reiser, *Adv. Funct. Mat.* 2014, **24**, 2020-2027.

28 Y. Xu, H. Bai, G. Lu, C. Li and G. Shi, *J. Am. Chem. Soc.* 2008, **130**, 5856–5857.

29 K. S. Kim, P. Tarakeshwar and J. Y. Lee, *Chem. Rev.* 2000, **100**, 4145-4186.

30 K. Jasuja and V. Berry, *ACS Nano*. 2009, **3**, 2358-2366.

31 C. Xu, X. Wang and J. Zhu, *J. Phys. Chem. C* 2008, **112**, 19841-19845.

32 V. Georgakilas, D. Gournisb, V. Tzitziosa, L. Pasquato, D. M. Guldie and M. Prato, *J. Mater. Chem.* 2007, **26**, 2679-2694.

33 H. P. Cong, J. J. He, Y. Lu and S. H. Yu, *Small* 2010, **6**, 169-173.

34 Y. M. Li, L. H. Tang and J. H. Li, *Electrochem. Commun.* 2009, **11**, 846-849.

35 C. Xu, X. D. Wu, J. W. Zhu and X. Wang, *Carbon* 2008, **46**, 386-389.

36 Joint Committee on Powder Diffraction Standards, Diffraction Data File: JCPDS International Center for Diffraction Data: Swarthmore, PA, 1991.

37 F.Y. Zhao, B. L. Zhang and L.Y. Feng, *Mater. Lett.* 2012, **68**, 112-114.

38 X. Zhang, Y. G. Niu, X. D. Meng, Y. Li and J. P. Zhao, CrystEngComm, 2013, **15**, 8166–8172

39 Z. C. Ma, H. Q. Yang, Y. Qin, Y. J. Hao and G. Li, *J. Mol. Catal. A: Chem.* 2010, **331**, 78–85.

40 A.S. Guram, X.H. Bei and H.W. Turner, *Org. Lett*. 2003, **5**, 2485–2487

41 B. Karimi, H. Behzadnia, M. Bostina and H. Vali. *Chem. Eur. J.* 2012, **18**, 8634-8640

42 R. R. Sever and T.W. Root, *J. Phys. Chem. B* 2003, 107, 4080-4089.

43 N. Dimitratos, A. Villa, D. Wang, F. Porta, D. Su and L. Prati, *J. Catal.* 2006, **244**, 113−121.

44 H. A. Rass, N. Essayem and M. Besson, *Green Chem.* 2013, **15**, 2240–2251.

45 A. Villa, M. Schiavoni, S. Campisi, G. M. Veith, L. Prati, *ChemSusChem*, 2013, **6**, 609-612.